Pergamon

Cement and Concrete Research, Vol. 28, No. 2, pp. 285–297, 1998
Copyright © 1998 Elsevier Science Ltd
Printed in the USA. All rights reserved
0008-8846/98 $19.00 + .00

PII S0008-8846(97)00264-0

PREDICTION OF ADIABATIC TEMPERATURE RISE IN CONVENTIONAL AND HIGH-PERFORMANCE CONCRETES USING A 3-D MICROSTRUCTURAL MODEL

D.P. Bentz,* V. Waller,† and F. de Larrard[1]†

*Building and Fire Research Laboratory, Building 226 Room B-350, National Institute of Standards and Technology, Gaithersburg, MD 20899

†Laboratoire Central des Ponts et Chaussees, 58, bd Lefebvre, 75732 Paris Cedex 15, France

(Received July 25, 1997; Accepted December 1, 1997)

ABSTRACT

A series of conventional and high-performance concretes, with and without silica fume additions, have been prepared and characterized with respect to their adiabatic heat signature. The measured responses are compared with predicted values from the NIST 3-D cement hydration and microstructural model, which has been modified to incorporate the pozzolanic reaction of silica fume and to simulate hydration under adiabatic conditions. The latter modification is based on the activation energies and heats of reaction for the hydration and pozzolanic reactions and the heat capacity of the hydrating concrete mixture. For concretes with and without silica fume, the agreement between predicted and measured response is always within about five degrees Celsius. For concretes with silica fume, using an appropriate stoichiometry for the pozzolanic C-S-H is critical in matching the long-term (4 to 8 day) experimental temperature rise behavior. © *1998 Elsevier Science Ltd*

Introduction

Cement hydration reactions are exothermic in nature, so that in an insulated system, the heat released during hydration will result in a measurable temperature rise. In high-performance concretes, due to the presence of silica fume and the generally higher cement contents, these temperature rises can result in serious thermal cracking problems (1). The ability to predict the expected temperature increase would thus be useful to structural engineers and designers interested in producing a durable concrete structure.

One approach for achieving this goal is to prepare a trial mixture of the concrete of interest and monitor its temperature rise when hydrated under adiabatic conditions. Another approach is to use a computer model to predict this temperature rise behavior. This paper describes both approaches for a variety of concretes with and without silica fume additions. A three-dimensional microstructural model has been modified to predict the adiabatic response

[1]To whom correspondence should be addressed.

TABLE 1
Materials used in concrete mixtures.

coarse aggregate	crushed limestone
sand	crushed limestone
cement	C2: CEM I 52.5 PM CP2 (Montalieu[a])
silica fume	Pechiney (Laudun)
superplasticizer	Sikament HR401 (Sika)

[a] This and other tradenames and company products are identified to adequately specify the experimental procedure. In no case does such identification imply endorsement by the National Institute of Standards and Technology, nor does it imply that the products are necessarily the best available for the purpose.

of a user-specified concrete mixture. Input data for the model, such as kinetic constants, heats of reaction, and activation energies, have been obtained from the literature or experiments employing the materials examined in this study.

Experimental Procedure

Concrete Mixture Testing

The materials for the concrete mixtures are given in Table 1. The chemical compositions of the cement and silica fume are provided in Table 2. The calculated Bogue composition (mass fractions) for the cement is 57.1% C_3S, 15.3% C_2S, 7.7% C_3A, and 8.4% C_4AF.

Concretes containing no silica fume and having different water-to-cement (w/c) ratios on a mass basis were produced. Based on some of these compositions, several series of silica

TABLE 2
Chemical composition in mass fraction (%) of cement and silica fume.

Compound/Cement Notation	Cement	Silica fume
SiO_2/S	20.4	87.0
CaO/C	62.6	0.4
Al_2O_3/A	4.7	0.3
TiO_2	0.3	0.0
Fe_2O_3/F	2.8	0.7
MgO	1.9	1.6
Na_2O	0.2	0.7
K_2O	0.9	2.4
SO_3/$\bar{S}$	2.7	0.3
Cl	–	0.3
MnO	0.0	0.1
LOI	1.9	3.1
Si	–	3.3

TABLE 3
Mixture proportions for concretes without silica fume.

w/c	0.30	0.35	0.45	0.55	0.65
Aggregates (kg)	1748.3	1821.0	1731.3	1859.7	1912.9
Cement (kg)	529.5	455.3	438.1	330.7	274.7
Superplasticizer (kg)	5.82	2.96	0.0	0.0	0.0
Total water (kg)	158.9	159.3	197.3	181.6	178.6

fume concretes with increasing silica fume-to-cement (s/c) mass ratios were made. The mixtures were designed to be workable using a plasticizer. For some mixtures, the paste volume was limited in order to keep the sample temperature below the maximum critical temperature of the calorimeters (around 80°C). The mixture proportions are given in Tables 3 and 4.

Before mixing, the materials were placed in a room having a regulated temperature equal to that of the adiabatic calorimeter to ensure thermal equilibrium at the beginning of the test. Immediately after mixing (within 5 to 8 min), a sample was put into the calorimeter. The calorimeter was designed to maintain the temperature of the casing surrounding the sample at the same temperature as the sample. The temperature and corresponding heat balance were

TABLE 4
Mixture proportions for concretes with silica fume.

w/c	0.30	0.30	0.30	0.35
s/c	0.05	0.10	0.30	0.20
Aggregates (kg)	1800.4	1752.6	1679.9	1785.5
Cement (kg)	474.8	483.9	453.2	453.0
Silica fume (kg)	23.7	48.4	136.0	90.6
Superplasticizer (kg)	5.7	0.0	0.0	0.0
Total water (kg)	142.4	145.2	136.0	158.5
w/c	0.45	0.45	0.45	0.45
s/c	0.05	0.10	0.20	0.30
Aggregates (kg)	1671.0	1883.6	1874.1	1815.4
Cement (kg)	455.3	344.1	323.3	333.8
Silica fume (kg)	22.8	34.4	64.7	100.1
Superplasticizer (kg)	0.0	4.1	5.8	6.7
Total water (kg)	204.9	154.8	145.5	150.2
w/c	0.55	0.65	0.65	0.65
s/c	0.20	0.05	0.10	0.30
Aggregates (kg)	1843.7	1879.2	1815.2	1771.7
Cement (kg)	307.2	281.9	300.2	295.1
Silica fume (kg)	61.4	14.1	30.0	88.5
Superplasticizer (kg)	0.0	0.0	0.0	0.0
Total water (kg)	168.9	183.1	194.9	191.8

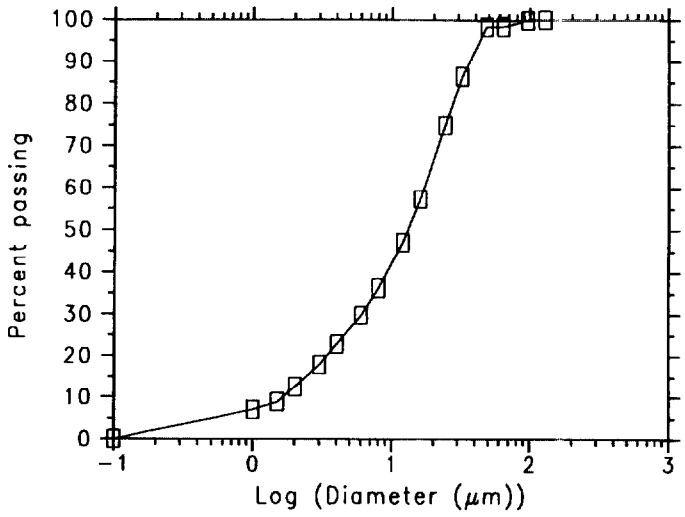

FIG. 1.
Measured particle size distribution for Montalieu cement.

maintained by an electrical regulator controlling an electrical-resistance heater. In general, the temperature of the concrete sample was recorded over several days.

Microstructural Modelling

A sample of the Montalieu cement was imaged using scanning electron microscopy/X-ray analysis (2) to obtain a two-dimensional image in which each phase of the cement was uniquely identified. This image, along with the measured particle size distribution for the cement (Fig. 1), was used in reconstructing a three-dimensional representation of the cement at each w/c ratio (3,4).

The cellular automaton-based 3-D cement hydration and microstructural model has been described in detail in a number of recent publications (3–5). The model operates as a sequence of cycles, each consisting of dissolution, diffusion, and reaction steps. To calibrate the model kinetics for this particular cement, experimental hydration tests were conducted under saturated conditions for w/c = 0.35 at a constant temperature of 25°C. Degree of hydration was quantified based on measurement of the non-evaporable water content (W_N) using loss on ignition techniques (3). Figure 2 presents the experimental data and model calibrated results for degree of hydration vs. time. Here, model dissolution cycles were converted to time, t, in hours using the equation:

$$t(model, h) = t_0 + \beta \times cycles^2 \quad (1)$$

where t_0 is the induction time (7.5 h) and β is a calibration constant, determined to be 0.0011 ± 0.0001 (one standard deviation) for this particular data set, based on analysis using the parabolic kinetic model of Knudsen (6). Following this calibration, excellent agreement was observed between the model and experimentally measured degrees of hydration over the full range of the 90-day study.

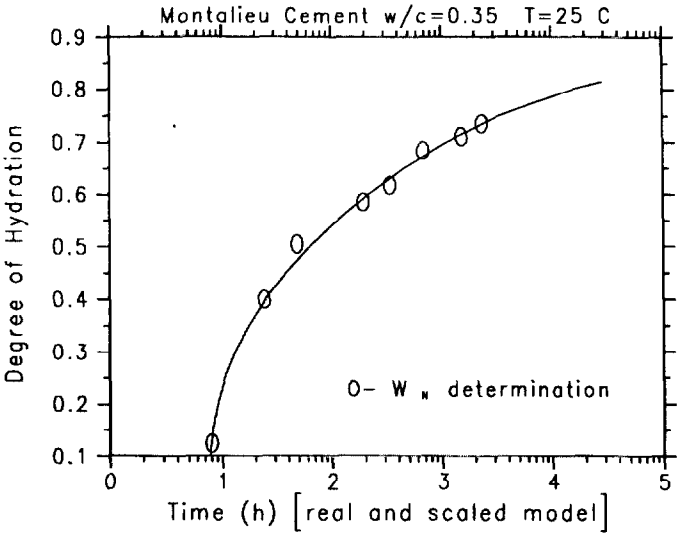

FIG. 2.
Comparison of experimental (data points) and simulated (solid lines) degree of hydration vs. time curves.

For the concretes examined in this study, curing was conducted under sealed conditions. Thus, the microstructural model was also executed under self-desiccating conditions, in which empty pore space is created as the hydration proceeds (4). Based on the volume stoichiometry of all hydration reactions, the computer model tabulates the current pore volume and the volume of water not yet consumed by reactions, with the chemical shrinkage being the difference between these two quantities. After each cycle of the hydration, the appropriate volume of capillary porosity is converted from being water-filled to being empty, emptying the "pores" from largest to smallest in an attempt to simulate the physical process. For w/c ratios of 0.4 and lower, curing under sealed conditions will result in significantly less hydration being achieved than equivalent curing under saturated conditions, due to the lack of capillary water available to continue the hydration at later ages (7).

To modify the NIST hydration model to operate under adiabatic conditions, the cumulative heat generated by the hydration reactions is tabulated and the heat capacity of the concrete mixture adjusted for the effects of hydration. The heats of reaction used for the individual cement clinker phases and silica fume are provided in Table 5, while the heat capacities of various components of a concrete mixture are provided in Table 6. As hydration occurs, the overall heat capacity of the concrete mixture decreases by about 5% as free water is bound into the hydration products.

Knowing the heat released during a given cycle of the hydration and the current heat capacity, an incremental temperature rise from cycle $(i - 1)$ to cycle i can be calculated as:

$$\Delta T = \frac{[H(i) - H(i-1)]}{C_p(i)} \tag{2}$$

where ΔT is the incremental change in temperature, $C_p(i)$ is the heat capacity of the concrete after cycle i, and $H(i)$ is the cumulative heat generated by the hydration reactions through

TABLE 5
Enthalpy of complete hydration for major phases of cement.

Phase	Enthalpy (kJ/kg phase)	Source
Tricalcium silicate	517	(8)[a]
Dicalcium silicate	262	(8)
Tricalcium aluminate	1144	(8)
Tetracalcium aluminoferrite	725	(9)[b]
Silica fume	780	(1)

[a] w/c = 0.4 and T = 21°C
[b] w/c = 0.5 and T = 20°C

cycle i. To compare the model to experimental results, one must calculate the equivalent time elapsed during a given cycle, making use of the principles of the maturity method (10).

Based on Eq. 1, the differential time elapsing between cycles $(i - 1)$ and i can be determined as:

$$\Delta t(i) = (2 \times i - 1) \times \beta. \tag{3}$$

This increment in time would correspond to a constant reaction temperature of 25°C, the temperature at which the model calibration was performed. To use the maturity method to determine the equivalent time at a different temperature, the variation in reaction rate, k_T, with temperature is described by an Arrhenius function (10):

$$k_T = k_0 \times e^{\frac{-E_a}{RT}} \tag{4}$$

where k_0 is a pre-factor, E_a is the apparent activation energy, R is the universal gas constant (8.314 J/(mol K)) and T is absolute temperature in K. For the Montalieu cement, an activation energy of 45.7 kJ/mol was determined experimentally. Using the Arrhenius relationship, an equivalent time, t_e, at any temperature of interest, T_i, relative to a reference temperature, T_r, can be calculated as:

$$t_e = \frac{k_T}{k_r} \times t = e^{\frac{-E_a}{R} \times \left(\frac{1}{T_i} - \frac{1}{T_r}\right)} \times t \tag{5}$$

TABLE 6
Heat capacities of concrete components (1)

Component	Heat Capacity (J/(g °C))
Siliceous Aggregate	0.75
Limestone Aggregate	0.84
Cement	0.75
Silica Fume	0.75
Water	4.18
Bound Water	2.2

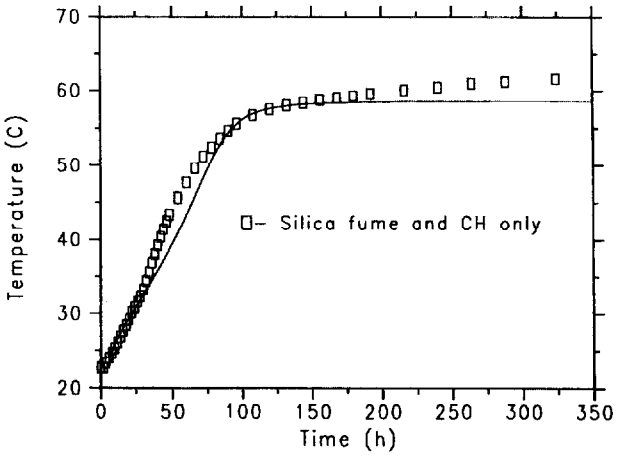

FIG. 3.
Comparison of experimental (*data points*) and simulated (*solid lines*) temperature rise curves for system containing only silica fume and CH.

where k_T is the rate constant at the current temperature of interest and k_r is the rate constant at the reference temperature. By combining Eqs. 3 and 5, one can determine the elapsed equivalent time at the current temperature, Δt_e, as:

$$\Delta t_e(i) = (2 \times i - 1) \times \beta \times \frac{k_T(\mathrm{i})}{k_r}. \tag{6}$$

Thus, as the microstructural model executes, Eqs. 2 and 6 are used to update the temperature and elapsed time, respectively. In addition, an induction time and initial temperature must be specified prior to model execution.

To model concretes containing silica fume, it was necessary to further modify the microstructural model to incorporate the pozzolanic reaction between calcium hydroxide (CH) and silica fume (S). Based on the results of Atlassi (11) and Lu et al. (12), the following reaction was used to represent the pozzolanic reaction:

$$1.1\mathrm{CH} + \mathrm{S} + 2.8\mathrm{H} \rightarrow \mathrm{C}_{1.1}\mathrm{SH}_{3.9} \tag{7}$$

Based on molar volumes of 27 cm^3/mol for silica, 33.1 cm^3/mol for CH, and 18 cm^3/mol for water, and assuming a molar volume of 101.81 cm^3/mol for pozzolanic C-S-H, one can compute a chemical shrinkage of 0.20 g H_2O/g silica fume. This value agrees with the range of values of 0.15-0.24 g H_2O/g silica fume measured by Jensen (13). Lu et al. (12) have observed a reduction in the H/S ratio of the pozzolanic C-S-H from 3.9 to 2.1 in going from 3 days to 28 days. Here, we have elected to use the constant value of 3.9 as it provides a better fit to the 4- to 8-day temperature rise of the concretes investigated experimentally. Also, based on the analysis of experimental data, an activation energy of 83.14 kJ/mol was determined for this pozzolanic reaction, which agrees with the value of approximately 80 kJ/mol measured by Jensen (13). This activation energy was further validated by using the microstructural model to simulate the temperature-time response of a system containing only calcium hydroxide crystals, silica fume particles, and water, as shown in Figure 3. While

TABLE 7
Ultimate degrees of hydration for various w/c and s/c under sealed curing conditions.

w/c	s/c	Ultimate degree of hydration	Fraction silica fume reacted
0.30	0.0	0.66 (0.61)	—
0.35	0.0	0.74 (0.67)	—
0.45	0.0	0.83 (0.76)	—
0.55	0.0	0.87 (0.82)	—
0.65	0.0	0.87 (0.87)	—
0.30	0.05	0.62 (0.58)	0.66 (0.59)
0.30	0.10	0.57 (0.55)	0.59 (0.53)
0.30	0.30	0.48 (0.53)	0.37 (0.33)
0.35	0.20	0.59 (0.59)	0.53 (0.48)
0.45	0.05	0.80 (0.73)	0.88 (0.79)
0.45	0.10	0.77 (0.71)	0.77 (0.69)
0.45	0.20	0.72 (0.68)	0.63 (0.56)
0.45	0.30	0.68 (0.68)	0.50 (0.45)
0.55	0.20	0.78 (0.74)	0.74 (0.67)
0.65	0.05	0.88 (0.85)	0.94 (0.85)
0.65	0.10	0.85 (0.83)	0.92 (0.83)
0.65	0.30	0.81 (0.79)	0.64 (0.58)

some minor differences exist at intermediate times, the overall agreement seems to suggest that a reasonable value is being employed for the activation energy in the model. The increased slope of the experimental temperature curve at intermediate times may be due to the presence of a size distribution of silica fume particles, not accounted for in the simulation.

In the microstructural model, silica fume particles are modelled as one pixel (1 μm) elements. Because the silica fume used in this study was only about 90% SiO_2, 10% of the silica fume was added as inert particles, which do not participate in any chemical reactions. This 90% "efficiency" for the silica fume is also in agreement with the measured long-term calcium hydroxide content present in the w/c = 0.45 concrete containing a 5% silica fume addition. To incorporate the above pozzolanic reaction into the model, calcium hydroxide crystals, which form at any point in the hydration, remain soluble, so that they may gradually dissolve over time, generating diffusing calcium hydroxide species that can then react at all silica fume surfaces. When there is no silica fume present in the system or when all of the silica fume present has been consumed, CH diffusing species simply reprecipitate on CH crystals, resulting in the Ostwald ripening of larger crystals at the expense of the smaller ones. The activation energy of the pozzolanic reaction, relative to that for the hydration of the cement, is used to change the probability of a reaction occuring when a diffusing CH species encounters a solid silica fume surface. This probability is adjusted with increasing temperature based on the ratio of the relative increase in the pozzolanic reaction rate to the relative increase in the hydration reaction rate, both calculated based on Eq. 4. In addition, the solubility (dissolution probability) of CH is adjusted with temperature according to the data provided in (8), which indicates about a 25% decrease in solubility as temperature increases from 25°C to 60°C.

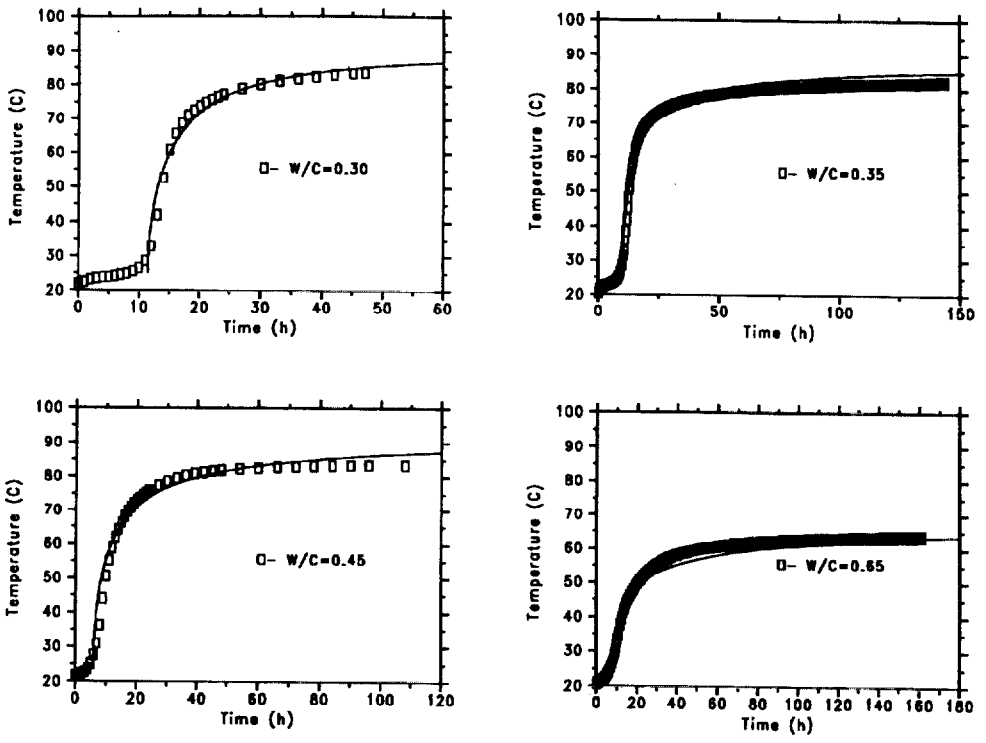

FIG. 4.
Comparison of experimental (*data points*) and simulated (*solid lines*) adiabatic heat signature curves for concretes without silica fume.

Results and Discussion

For each concrete, 5000 cycles (corresponding to about 3 years at 25°C) of hydration were executed using the microstructural model. The "final" degrees of hydration achieved using the model are summarized in Table 7. For ultimate degree of hydration, the values in parentheses indicate the values estimated for 28 days of hydration based on equations developed by Waller et al. (1). Except for the w/c = 0.3, s/c = 0.3 concrete, the 3-year values are consistently higher than the 28-day values, as would be expected. Also, a reduction in w/c ratio below 0.55 is seen to significantly reduce the achievable hydration, due to both a decrease in the available pore space to be filled by hydration products and self-desiccation effects. The presence of silica fume is seen to further reduce the ultimate achievable hydration, as extra water is incorporated into the pozzolanic reaction products and is thus unavailable for participating in the cement hydration reactions.

Table 7 also gives the volume fraction of the reactive silica fume that had reacted after the 5000 cycles of hydration, with the values in parentheses being the volume fraction of all of the silica fume, including the 10% of the silica fume that was initially assigned to be inert. The values for the higher silica fume additions can be compared to those measured via nuclear magnetic resonance analysis by Sun and Young for densified with small particles (DSP) pastes (14). For silica fume replacements between 18% and 48%, these researchers

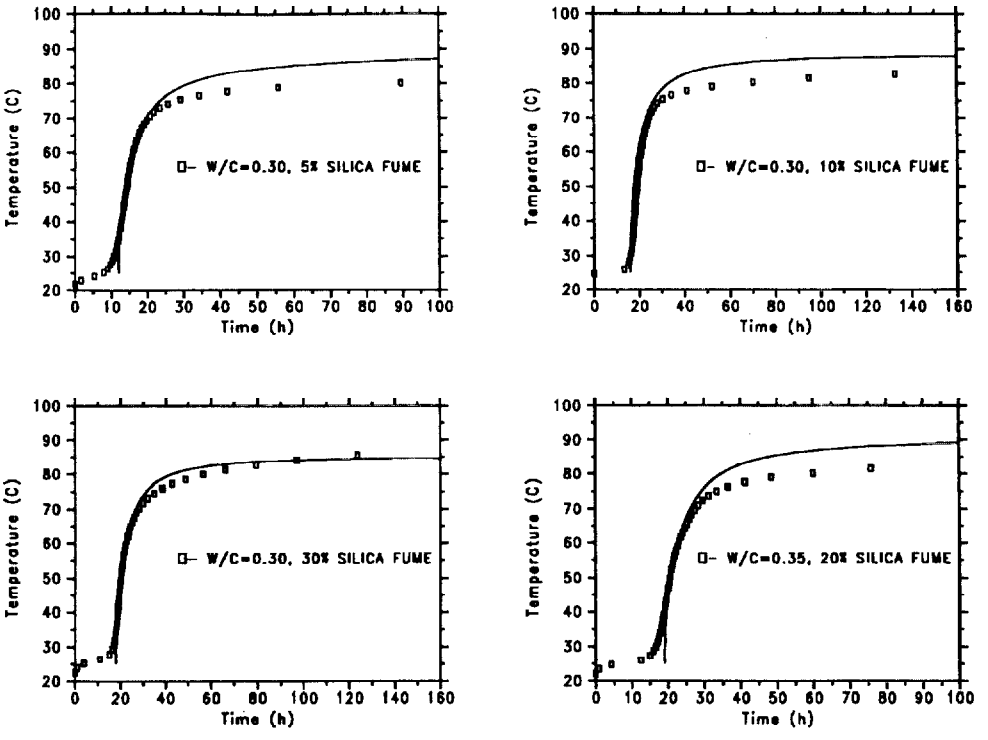

FIG. 5.
Comparison of experimental (*data points*) and simulated (*solid lines*) adiabatic heat signature curves for low w/c ratio concretes with silica fume.

determined that between 54% and 60% of the silica fume had reacted after 180 days, in general agreement with the model values of between 37% and 66% for the lower w/c ratio concretes.

Figure 4 provides a comparison of the experimental and model adiabatic temperature rise curves for a series of concretes without silica fume. By adjusting the induction time and the initial system temperature in the model, a reasonably good agreement is obtained between the model and experimental results. These results suggest that the model could be employed to simulate the adiabatic response of a wide variety of concretes, provided that the component materials had been characterized as performed in this study.

For the concretes containing silica fume, as shown in Figures 5 through 7, the agreement is also quite reasonable. Interestingly, for the higher w/c ratio concretes, there is some deviation between model and experiment at intermediate times, as was observed for the system containing only silica fume and calcium hydroxide in Figure 3. Because of the large amount of water (chemically bound and gel) incorporated into the pozzolanic C-S-H gel, the hydration effectively terminates at a much lower degree of hydration when curing is conducted under sealed conditions. If an H/S ratio of 2.1, as opposed to 3.9, is used in representing the pozzolanic C-S-H stoichiometry, the model-predicted temperature rise significantly exceeds the experimental values at times greater than 30 h, as sufficient water remains to continue the hydration. One of the complications in the modelling of cement-

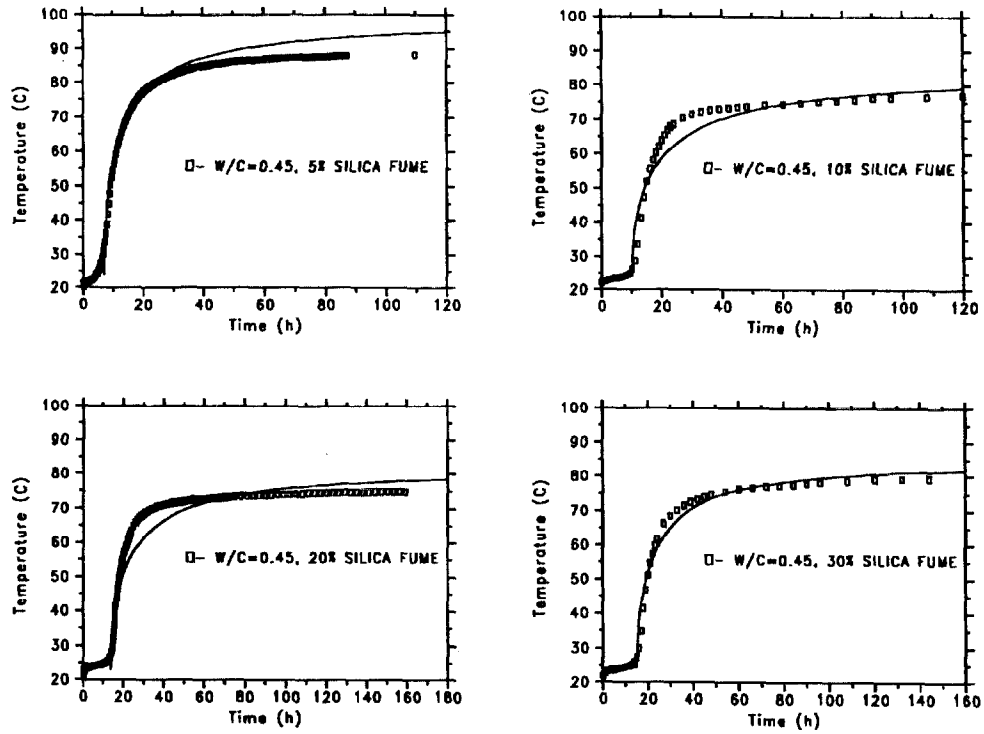

FIG. 6.
Comparison of experimental (*data points*) and simulated (*solid lines*) adiabatic heat signature curves for intermediate w/c ratio concretes with silica fume.

based materials is that the C-S-H gel (primary and pozzolanic) creeps and polymerizes over time (12,15), expelling gel water that can then participate in further hydration reactions. However, based on these results, for the purposes of predicting the early temperature rise behavior of a concrete, the use of a constant stoichiometry to represent the C-S-H appears to be reasonable.

Conclusions

The NIST 3-D microstructural model has been used successfully to predict the adiabatic temperature rise of a variety of concrete mixtures. Once the model was supplied with the proper kinetics constants, activation energies, and reaction product (e.g., pozzolanic C-S-H) stoichiometries, the agreement between model and experimental temperature rise vs. time curves was quite reasonable for all of the different mixture proportions examined. In addition to the temperature rise prediction, the model also provided estimates of the ultimate achievable degree of hydration for curing under saturated or sealed conditions, as well as the proportion of the silica fume that will react for a given set of mixture proportions. Currently, the model cannot predict the induction period, which limits its application in predicting early age concrete strength development. On the other hand, the prediction of hydration heat,

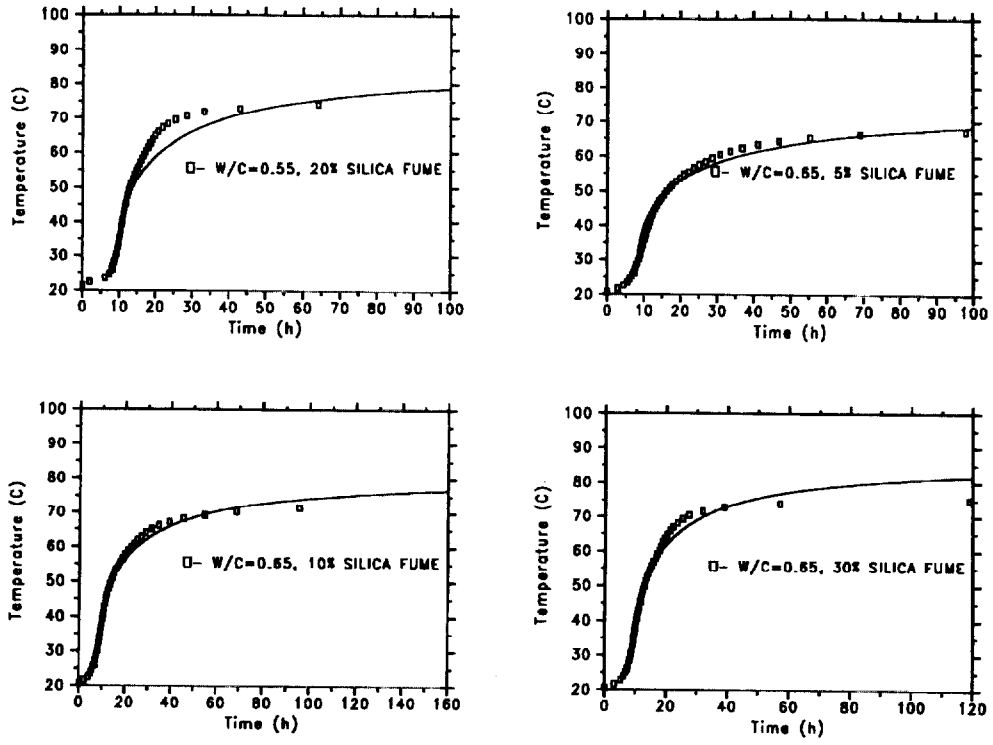

FIG. 7.
Comparison of experimental (*data points*) and simulated (*solid lines*) adiabatic heat signature curves for high w/c ratio concretes with silica fume.

which certainly influences the propensity for cracking of a concrete structure, can be accurately simulated, with any mixture produced with an already characterized (heat capacities, kinetic constants, etc.) set of constituents.

Acknowledgments

The experimental measurements were completed as a part of a Ph.D. thesis by one of the authors, V. Waller, who would like to thank Electricite de France and Leon Grosse for partial funding of his research.

References

1. V. Waller, F. de Larrard, and P. Roussel, 4th Int. Symp. Utilization of High-Strength/High-Performance Concrete, RILEM, pp. 415–421, May 1996.
2. D.P. Bentz and P.E. Stutzman, SEM analysis and computer modelling of hydration of Portland cement particles. Petrography of Cementitious Materials, S.M. DeHayes and D. Stark (eds.) pp. 60–73, ASTM, Philadelphia, PA, 1994.
3. D.P. Bentz, A Three-Dimensional Cement Hydration and Microstructure Program. I. Hydration

Rate, Heat of Hydration, and Chemical Shrinkage, NISTIR 5756, U.S. Department of Commerce, November 1995.
4. D.P. Bentz, J. Am. Ceram. Soc., 80, 3–21 (1997).
5. D.P. Bentz, Guide to Using CEMHYD3D: A Three-Dimensional Cement Hydration and Microstructure Development Modelling Package, NISTIR 5977, U.S. Department of Commerce, February, 1997.
6. T. Knudsen, Cem. Concr. Res., 14, 622–630 (1984).
7. D.P. Bentz, K.A. Snyder, and P.E. Stutzman, Proc. 10th Int. Congr. Chem. Cem. 2, 2ii078 (1997).
8. H.F.W. Taylor, Cement Chemistry, Academic Press, Inc., London, 1992.
9. M. Fukuhara, S. Goto, K. Asaga, K. Daimon, and R. Kondo, Cem. Concr. Res. 11, 407–414 (1981).
10. N.J. Carino, L.I. Knab, and J.R. Clifton, Applicability of the Maturity Method to High-Performance Concrete, NISTIR 4819, U.S. Department of Commerce, May 1992.
11. E.H. Atlassi, A Quantitative Thermogravimetric Study on the Nonevaporable Water in Mature Silica Fume Concrete, Ph. D. Thesis, Chalmers University of Technology, Goteborg, August 1993.
12. P. Lu, G.K. Sun, and J.F. Young, J. Am. Ceram. Soc. 76, 1003–1007 (1993).
13. O.M. Jensen, The pozzolanic reaction of silica fume (in Danish), TR 229/90, Building Materials Laboratory, Technical University of Denmark, 1990.
14. G.K. Sun and J.F. Young, Cem. Concr. Res. 23, 480–483 (1993).
15. A. Bentur, R.L. Berger, F.V. Lawrence, Jr., N.B. Milestone, S. Mindess, and J.F. Young, Cem. Concr. Res. 9, 83–96 (1979).